

Contribution of Spatially and Spectrally Resolved Cathodoluminescence to Study Crack-Tip Phenomena in Silica Glass

Giuseppe Pezzotti* and Andrea Leto

Ceramic Physics Laboratory & Research Institute for Nanoscience, Kyoto Institute of Technology

Sakyo-ku, Matsugasaki, 606-8585 Kyoto, Japan

(Received 28 April 2009; published 23 October 2009)

A current controversy over the nature of fracture in silica glass is revisited in the light of additional experimental evidence obtained by cathodoluminescence (CL) spectroscopy in the immediate crack-tip zone of two different types of silica glass. The Letter describes the dual experimental output obtained by monitoring optically active oxygen defects in silica glass, as follows: (i) analysis of local crack-tip stoichiometry (i.e., lattice defect population); and, (ii) spatially resolved stress analysis ahead of the crack tip based on a piezo-spectroscopic (PS) approach. CL experiments provided us with direct access to crack-tip stress fields, thus unfolding some missing detail about the complex mechanochemical interactions occurring at the crack tip in silica glass.

DOI: 10.1103/PhysRevLett.103.175501

PACS numbers: 62.20.M-, 46.50.+a, 61.43.Fs, 78.60.Hk

I. Introduction.—In the engineering practice, estimates of environmental effects on the fracture behavior of silica glass have been long and systematically pursued according to macroscopic strength data collected under different environmental conditions [1,2]. The issue is relevant to understand the basic structure of glass, its interaction with the fracture path and, ultimately, the possibility of extending the functionality of glass into new areas. Studies show that crack-tip fracture mechanisms in silica glass are indeed severely affected by the chemical environment, but also hint that such an interaction is confined to a scale in the order of individual atomic bonds [3,4]. It should be noted that high-resolution stress assessments in silica glass are hardly achievable, due to a lack of a stress sensor in its amorphous structure. For example, no researcher has so far succeeded in the direct measurements of crack-tip stress in silica glass with nanometer-scale spatial resolution. The debate on the intrinsic nature of fracture in silica glass has recently gained renewed interest due to straightforward (but somewhat difficult to interpret) experimental outcomes obtained by atomic force microscopy (AFM). Guin and Wiederhorn [5] examined the topography of fracture surfaces on the scale of the single nanometer and found no evidence for cavitation zone down to a size of 5 nm. These data support the view of an atomically sharp crack propagation (i.e., an Irwin-like [6] stepwise “elastic rupture of interatomic bonds”), but leave it open to debate the possibility of lattice trapping, involving local crack instability (i.e., accompanied by atomic-scale crack-path deflection) in the amorphous network. On the other hand, Célarié *et al.* [7] suggested the occurrence of “ductile” fracture behavior on the nanometer scale for silica glass, which arises from the presence of a damage/cavity zone as large as ≈ 20 nm ahead of the crack tip. The fracture mode envisaged by these latter researchers can be classified with

reference to the Hillerborg model of fracture in semibrittle solids [8], according to which a damage zone exists ahead of the crack tip and blunts it during propagation.

With this background in mind, we attempt here an interpretation of the intrinsic fracture behavior of silica glass based on a spatially resolved CL analysis. This method exploits the optical activity of nonstoichiometric sites in the amorphous network and uses it as a sensor for stress analysis. A highly focused electron probe impinges on the glass surface with a low acceleration voltage (i.e., ≤ 6 kV) and stimulates the CL emission. CL spectroscopy enables direct access to the trace of the stress tensor with a raw resolution of the hundredth of nm. However, the exact knowledge of the Gaussian nature of the CL probe offers the possibility to wipe out averaging effects by a mathematical deconvolution routine, thus restoring the actual stress distribution. The CL approach probably represents the only actual alternative to AFM scanning in directly tackling the problem of crack-tip fracture in amorphous silica from a microscopic point of view.

II. Experimental technique.—Two high-purity silicon oxide materials were investigated: one was a conventional high-purity fused silica (OP Grade, Tosoh Co., Tokyo, Japan), whose surface was finely polished and subsequently annealed; the other was a specially manufactured strain-free high-purity fused silica glass (ES Grade, Tosoh Co., Tokyo, Japan). These two materials will be henceforth simply referred to as “fused silica” *A* and *B*, respectively. A further type of silica sample, with a completely different stoichiometry, could be obtained from a large and thick pool of silica glass contained in trenches of an advanced silicon-on-insulator structure. This latter glass was prepared by low-pressure chemical vapor deposition of tetraethoxysilane (TEOS) oxide deposited at 700 °C and further annealing at 1050 °C. This latter type of glass will be

simply referred to as “TEOS silica”, henceforth. Vickers indentations were produced in ambient atmosphere on the silica surface using a force of 5 N applied for 10 s. The print produced half-penny-shaped cracks propagating from the corners of the print, whose tips were analyzed by CL spectroscopy.

Details of the CL technique applied to various kinds of silica glass have been extensively reported in previous publications [9–11]. Briefly, we used a field-emission-gun scanning electron microscope FEG-SEM with Schottky-emission type gun (S-4300SE, Hitachi, Tokyo, Japan) as an excitation source. A high-sensitivity CL detector unit (MP-32FE, Horiba Ltd., Kyoto, Japan) was employed for the collection of light upon reflection into an ellipsoidal mirror and transmission through a bundle of optical fibers. The spectrum of the emitted light was analyzed using a highly precise monochromator (TRIAX 320, Jobin-Ivon-Spex) equipped with a liquid nitrogen cooled CCD camera. A mapping device (PMT R943-02 Select, Horiba Ltd., Kyoto, Japan) and related software were developed, which enabled point-grid collection with nanometer-scale spatial resolution and nearly real-time analysis of a large number of acquired spectra.

The electron probe was focused over the crack tip and precisely translated to scan along the crack path in the neighborhood of the crack tip. The area of electron impingement at each CL acquisition on the silica surface was confined to the order of few square nanometers, but electrons unavoidably scattered inside the amorphous structure, the larger their onionlike broadening the higher the selected acceleration voltage. A lower limit for acceleration voltage was dictated by the efficiency of the CL emission, which for defect emission in silica glass was unfortunately rather low and imposed a choice of beam voltage in the order of 3 (for the TEOS silica sample) to 6 kV (for both fused silica samples *A* and *B*). The diameter of the electron-irradiated zone then broadened up to 600 nm (at 6 kV). On the other hand, two experimental circumstances helped us in the experimental evaluation of the crack tip: (i) the sampling step along the line scan across the crack tip could be confined to few nanometers; and, (ii) the electron broadening was Gaussian in nature,

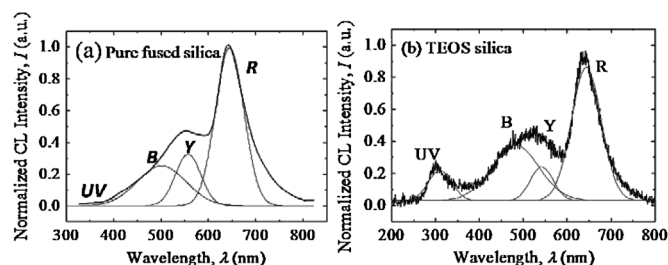


FIG. 1. Comparison between CL spectra collected under the same experimental conditions in zones far away from the crack tip in: (a) fused silica (no significant difference was found between sample *A* and *B*); and, (b) TEOS silica glass.

which enabled us to cancel out its convolutive effects by means of a mathematical deconvolution routine [9–11]. Spatial deconvolution was obtained by a mathematical routine that was built up in-house using commercially available software [*MATHEMATICA* 4, Wolfram Research Inc., IL, USA (2000)].

III. Experimental results.—Figures 1(a) and 1(b) show a comparison between the CL spectra collected under the same experimental conditions in zones far away from the crack tip in fused silica (no significant difference was found between sample *A* and *B*) and TEOS silica glasses, respectively. In both cases, the predominant feature in the CL spectrum is observed in the red region at about 640 nm (*R* band). This CL band is related to nonbridging oxygen hole centers (NBOHC), namely, the oxygen-excess sites of the glass network [12]. Another band of relevant intensity can be found in the blue region between 460 and 500 nm (band *B*), which instead arises from a population of two-fold coordinated silicon centers, thus generated in the presence of an oxygen vacancy site (i.e., an oxygen deficient center, ODC) [13]. A further band in the yellow region of the spectrum (band *Y*) arises from the presence of structural water [13], while the ultraviolet band located at about 290 nm (*UV* band) originates from ODC centers [13]. The relative intensity of the above bands reveals the local stoichiometry of the silica network and can be used for our present purpose of characterizing the local chemical state at the crack tip of silica glass. From simple considerations of glass stoichiometry, one would expect the presence of intrinsic water contributing to increase the intensity of both bands *Y* and *R*. A complication to this scenario arises from the fact that carbon impurities on the surface of silica also produce a rise in the CL spectrum of a band located around 530 nm, which is time dependent and partly overlap the band *Y* from structural water. On the one hand, this places a limitation on spectral accumulation time in CL experiments, because impinging a low-voltage electron beam for relatively long time on the surface of silica unavoidably involves local contamination by carbon.

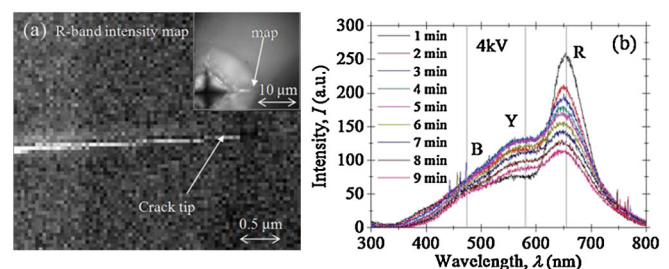


FIG. 2 (color). (a) Map of band *R* intensity collected in the neighborhood of the crack tip in fused silica. The crack-tip location is indicated in the map and it was retrieved from a SEM micrograph of the mapped area. A low-magnification map of *R*-band intensity is shown in the right-top corner inset. (b) CL spectral variation vs time as collected in fused silica just ahead of the crack tip.

However, this phenomenon can be used to confirm local changes in crack-tip stoichiometry under the electron beam, as shown hereafter. Figure 2(a) shows a map of band- R intensity collected in the neighborhood of the crack tip in fused silica. In the inset, a map of the same kind is shown as collected over a large portion of the entire indentation. In this experiment, a photomultiplier was used and the accumulation time could be kept as short as 100 ms per each probed location in the attempt of minimizing carbon contamination on the silica surface. Higher intensity was indeed found over a region of the order of hundreds of nanometers along the crack path and ahead of the crack tip, which could indeed be interpreted as due to the enhanced presence of structural water. In Fig. 2(b), CL spectral variation is shown, which was detected in the spectrum of fused silica collected just ahead of the crack tip (i.e., in the zone of stoichiometry change shown in Fig. 2(a)). With increasing irradiation time at a fixed location, the R band of oxygen-excess centers becomes conspicuously annihilated by the local formation of dangling bonds with contaminating carbon. This observation can be also interpreted as a process of water depletion. It should be also considered that long-term irradiation might lead to a local rise in temperature with consequent evaporation of water in the vacuum chamber of the microscope.

A PS approach applied to the band R enables the quantitative assessment of stress in silica glass [9–11]. The output of the PS assessment applied to point-defect luminescence is an estimate of the trace of the principal stress tensor [9–11,14]. Figures 3(a) and 3(b) show maps of such a stress trace in the neighborhood of the crack tip, as collected on fused silica A and B , respectively. The spatial resolution of the two maps is ≈ 200 nm. In conventional fused silica (sample A), the surface is dominated (i.e., even after annealing) by residual stress patterns developed on a mesoscopic scale. This makes the crack-tip stress field extremely scattered and irregular. On the other hand, in stress-free fused silica (sample B), the crack-tip stress field shows areas of local intensification but yet better symmetry and morphology, as typical of brittle materials. Because of the strong influence of surface residual stresses on the

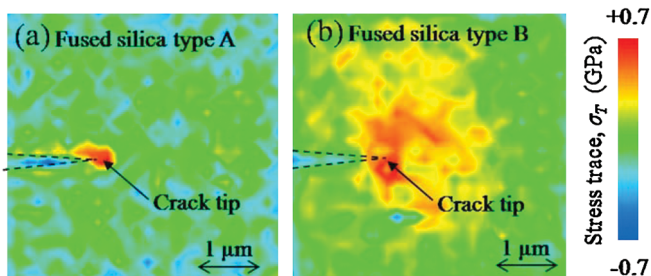


FIG. 3 (color). Quantitative assessment of the trace of the principal stress tensor in silica glass in the neighborhood of the crack tip, as collected on fused silica sample A and B , respectively.

crack-tip stress field, sample A was not investigated further. Linear plots of experimental crack-tip stress are shown in Figs. 4(a) and 4(b) for fused silica B and TEOS silica, respectively. The results of a mathematical probe-deconvolution procedure on the experimental stress profiles ahead of the crack tip are also shown in Figs. 4(a) and 4(b). A trial function was set according to the Irwin equation [6,15] in which the crack-morphology weight function was assumed as given by Fett [16] for half-penny-shaped indentation cracks. A detailed explanation of the crack-tip data treatment and of the related computational procedures is omitted here for brevity's sake, but it can be found in previously published papers [9–11]. The procedure locates K_I values of 0.70 and 0.13 $\text{MPa}\cdot\text{m}^{1/2}$ for silica sample B and TEOS silica, respectively. The crack-tip stress intensity results obtained by CL were confirmed according to a quantitative assessment of crack opening displacements from high-resolution FEG-SEM images according to a procedure suggested by Rödel and co-workers [17,18]. The stress intensity factors obtained from least-square fitting of the experimental COD data were $K_I = 0.68$ and 0.11 $\text{MPa}\cdot\text{m}^{1/2}$ for silica sample B and TEOS silica, respectively. These latter results, which were obtained by an independent experimental approach on the same cracks investigated by CL, show good agreement with the K_I values obtained by the PS method, thus confirming the validity of our CL stress assessments in silica glass. Furthermore, a lower-limit value for the actual magnitude of crack-tip stress in the highly graded part of the plots can be estimated by correcting the convolutive effects of electron broadening by means of a mathematical deconvolution routine that takes into consideration the Gaussian nature of the probe [19–21]. The maximum stress after probe deconvolution was in the order of several GPa (i.e., in the range 2.8–3.5 GPa) for both the investigated silica glasses [cf. maximum stress values $\sigma_{ii}^{(\text{max})}$ in the plateau of the full lines plots in Figs. 4(a) and 4(b)]. Such high crack-tip stress values locate an upper limit for the size of

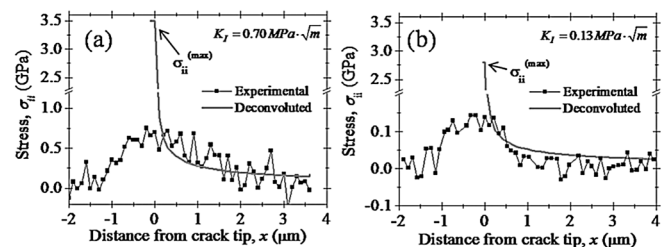


FIG. 4. Linear plots of crack-tip stress are shown in the K_I -dominated area for fused silica B (a) and TEOS silica (b), respectively. Each data plot is the average of 5 experimental points. The results of a mathematical probe-deconvolution procedure on the experimental stress profiles ahead of the crack tip are also shown. From these latter plots a maximum stress value, $\sigma_{ii}^{(\text{max})}$, at the crack tip was computed according to a procedure described in Ref. [21].

the crack-tip “plastic” zone that, thus, should be less than 6 nm for fused silica and below the single nanometer in TEOS silica, thus ruling out the presence of any relatively large plastic zone.

IV. Discussion and conclusions.—From the above results, we summarize that, within the limits of resolution and the conditions used in this study, there is no significant stress relaxation zone at the crack tip of the silica glasses that were studied. However, it should be noted that the present study necessarily offers partial results and call for a systematic investigation in a range of concentration for intrinsic water in silica glass. In this context, it should be noted that the investigated types of silica glass represent paradigm materials in the field. A gradient in stoichiometry was found at the crack tip of fused silica, which was clearly related to the crack propagation phenomenon and could be, in principle, attributed to a concentration of intrinsic water in the neighborhood of the crack tip (as already suggested by other authors [22]). In terms of crack-tip stress analysis, this study probably cannot give a final answer in unfolding the intrinsic strength of glass. This was due to difficulty in lowering the acceleration voltage of the electron probe, in turn related to a discrete nature of the stress sensor used. Improvements in spatial resolution would require the solution of CL efficiency issues for optically active defective sites in silica glass. Nevertheless, we clearly prove here the importance of considering, besides chemistry issues, the microscopic residual stress fields on the surface of silica glass. In addition, we report a direct evaluation of crack-tip stress fields with unprecedented spatial resolution for silica glass.

The subject of this Letter was inspired by conversations with Doctor S. M. Wiederhorn, Professor M. Tomozawa, Professor T. Rouxel, Professor C. Pantano, and Doctor M. Ciccotti during the EFONGA Meeting 2009 in Montpellier, France.

*Corresponding author.

- [1] C. R. Kurkjian, P. K. Gupta, R. K. Brown, and N. Lower, *J. Non-Cryst. Solids* **316**, 114 (2003).
- [2] B. A. Proctor, I. Whitney, and J. W. Johnson, *Proc. R. Soc. A* **297**, 534 (1967).
- [3] B. R. Lawn, B. J. Hockey, and S. M. Wiederhorn, *J. Mater. Sci.* **15**, 1207 (1980).
- [4] W. B. Hillig, *Microplasticity*, edited by C. J. McMahon (Interscience, New York, 1968), p. 383.
- [5] J.-P. Guin and S. M. Wiederhorn, *Phys. Rev. Lett.* **92**, 215502 (2004).
- [6] G. R. Irwin, *J. Appl. Mech.* **24**, 361 (1957).
- [7] F. Célerié, S. Prades, D. Bonamy, L. Ferrero, E. Bouchaud, C. Guillot, and C. Marlière, *Phys. Rev. Lett.* **90**, 075504 (2003).
- [8] A. Hillerborg, M. Modeer, and P. E. Petersson, *Cement and Concrete Research* **6**, 773 (1976).
- [9] A. Leto, A. A. Porporati, W. Zhu, M. Green, and G. Pezzotti, *J. Appl. Phys.* **101**, 093514 (2007).
- [10] A. Leto, M. C. Munisso, A. A. Porporati, W. Zhu, and G. Pezzotti, *J. Phys. Chem. A* **112**, 3927 (2008).
- [11] G. Pezzotti, A. Leto, and A. A. Porporati, *J. Ceram. Soc. Jpn.* **116**, 869 (2008).
- [12] L. Skuja, *J. Non-Cryst. Solids* **179**, 51 (1994).
- [13] R. Salh, B. Schmidt, and H. J. Fitting, *Phys. Status Solidi A* **202**, R53 (2005).
- [14] L. Grabner, *J. Appl. Phys.* **49**, 580 (1978).
- [15] H. Tada, P. C. Paris, and G. R. Irwin, *The Stress Analysis of Cracks* (Handbook Del. Research Corporation, Hellertown, PA, 1973).
- [16] T. Fett, Report No. FZKA 6757, Forschungszentrum Karlsruhe, Germany, 2002.
- [17] J. Rödel, J. Kelly, and B. R. Lawn, *J. Am. Ceram. Soc.* **73**, 3313 (1990).
- [18] Z. Burghard, A. Zimmermann, J. Rödel, F. Aldinger, and B. R. Lawn, *Acta Mater.* **52**, 293 (2004).
- [19] C. Donolato and P. Venturi, *Phys. Status Solidi A* **73**, 377 (1982).
- [20] W. Zhu, M. C. Munisso, A. Matsutani, W. Ge, and G. Pezzotti, *Appl. Spectrosc.* **63**, 185 (2009).
- [21] W. Zhu, A. A. Porporati, A. Matsutani, N. Lama, and G. Pezzotti, *J. Appl. Phys.* **101**, 103531 (2007).
- [22] M. Ciccotti, M. George, V. Ranieri, L. Wondraczek, and C. Marlière, *J. Non-Cryst. Solids* **354**, 564 (2008).